GMR
The Original

PHYSICOCHEMICAL CHARACTERIZATION AND ANTI-INFLAMMATORY POTENTIAL OF STARCH/PVA/CUO-NPS ELECTROSPUN NANOSCAFFOLDS FROM TURBINARIA ORNATA (MARINE MACROALGAE) EXTRACT

Martina Ainslay Paul Arul Raj[1], Anoosh Golla[2], Abyramy Balasundaram[3], Alagendran Subbarayalu[4], Kaliyamoorthy Dass[5*]

[1]Saveetha Medical College & Hospital (SMCH), Saveetha Institute of Medical and Technical Sciences (SIMATS), Thandalam, Chennai, Tamil Nadu 602105, India. Email: martinaainslay@gmail.com
[2]Department of Neurology, Saveetha Medical College and Hospital, Saveetha Institute of Medical And Technical Sciences (SIMATS), Thandalam, Chennai-602105, Tamil Nadu, India. Email: anushyadav2025@gmail.com
[3]Department of Dermatology, Saveetha Medical College and Hospital, Saveetha Institute of Medical And Technical Sciences (SIMATS), Thandalam, Chennai-602105, Tamil Nadu, India. Email: b.abyramy@gmail.com; ORCID: https://orcid.org/0000-0002-0534-6225
[4]Saveetha College of Nursing (SCON), Saveetha Institute of Medical and Technical Sciences (SIMATS), Chennai – 602105, Tamil Nadu, India. Email: alagendrans.scon@saveetha.com; ORCID: https://orcid.org/0009-0009-0749-7180
[5*]Natural Product and Vector Control Research Lab, Department of Pharmacology, Saveetha Medical College and Hospital, Saveetha Institute of Medical And Technical Sciences (SIMATS), Thandalam, Chennai-602105, Tamil Nadu, India. Email: dass.smc@saveetha.com; ORCID: https://orcid.org/0000-0002-4564-3275
*Corresponding Author: Email: dass.smc@saveetha.com

ABSTRACT

Background: This study explores the physicochemical characterization and anti-inflammatory potential of starch/polyvinyl alcohol/copper oxide nanoparticle (starch/PVA/CuO-NPs) nanoscaffolds synthesized using Turbinaria ornata marine macroalgae extract. UV-Visible spectroscopy confirmed the successful biosynthesis of CuO NPs, exhibiting a characteristic absorption peak at 200 nm, while the algal extract displayed a broad peak at 346 nm, indicative of bioactive phytoconstituents. Fourier-transform infrared (FTIR) analysis revealed functional groups corresponding to Cu–O bonds (601 cm^{-1}) and polymer matrix interactions (3284 cm^{-1}, O–H/N–H stretches). X-ray diffraction (XRD) confirmed the monoclinic crystalline structure of CuO NPs, while scanning electron microscopy (SEM) demonstrated uniform nanofiber morphology (150–300 nm) with well-dispersed NPs. Thermal stability was enhanced in nanoscaffolds, as evidenced by thermogravimetric analysis (TGA), with degradation onset at 244.81°C. Dynamic light scattering indicated an average NP size of 92.8 nm, though zeta potential (-5.29 mV) suggested moderate colloidal stability. Anti-inflammatory assays demonstrated concentration-dependent inhibition of protein denaturation and xanthine oxidase activity. At 100 µg/mL, nanoscaffolds exhibited the highest inhibition (79.21% for protein denaturation; 77.81% for xanthine oxidase), outperforming CuO NPs and algal extract, likely due to synergistic effects. These findings highlight the nanoscaffolds' superior anti-inflammatory efficacy, positioning them as promising candidates for biomedical applications. Further in vivo studies are warranted to validate their therapeutic potential.

KEYWORDS: Turbinaria ornata, Green synthesis, CuO nanoparticles, Starch/PVA nanoscaffolds, Anti-inflammatory activity.

1. INTRODUCTION

The integration of marine resources into biomedical applications has garnered substantial interest in recent years due to the rich repository of bioactive compounds found in marine organisms, particularly seaweeds [1]. Among these, Turbinaria ornata, a brown macroalga found abundantly along the Indian coastline, offers a valuable source of secondary metabolites with diverse therapeutic activities, including anti-inflammatory, antioxidant, antimicrobial, and anticancer properties [2]. These natural products, when harnessed effectively, can serve as potent agents for functionalizing nanomaterials, enhancing their biocompatibility and therapeutic efficacy [3]. Simultaneously, advancements in green nanotechnology have paved the way for eco-friendly synthesis of metal-based nanoparticles, using marine-derived extracts as reducing and stabilizing agents [4]. In this context, copper oxide nanoparticles (CuO-NPs) have emerged as attractive candidates due to their inherent antimicrobial, anti-inflammatory, and catalytic properties [5].

The biomedical relevance of CuO NPs is heightened by their ability to generate reactive oxygen species (ROS), modulate inflammatory responses, and interact with microbial membranes, leading to potential applications in wound healing, drug delivery, and tissue engineering [6]. However, the traditional chemical synthesis of CuO NPs often involves toxic solvents and harsh reducing agents, raising environmental and safety concerns [7]. The green synthesis approach using marine macroalgae such as T. ornata provides a sustainable alternative, where naturally occurring polyphenols, flavonoids, and

sulfated polysaccharides in the algal extract facilitate nanoparticle formation under mild reaction conditions [8]. This method not only ensures environmental compatibility but also contributes to the biological functionality of the resulting nanomaterials [9].

In parallel, the design of nanostructured scaffolds using biopolymeric matrices has become a focal point in regenerative medicine and drug delivery [10]. Electrospinning, a versatile technique for fabricating nanofibrous scaffolds, enables the production of structures that closely mimic the extracellular matrix (ECM), thereby enhancing cell adhesion, proliferation, and differentiation [11]. Polymers such as starch and polyvinyl alcohol (PVA) are commonly employed in electrospinning due to their biodegradability, non-toxicity, and ease of processing [12]. PVA, a synthetic polymer with excellent film-forming and mechanical properties, is often blended with natural biopolymers like starch to improve the mechanical integrity and physiological relevance of the scaffold [13]. The incorporation of bioactive nanoparticles such as CuO into the electrospun nanofiber matrix further augments the scaffold's functionality by endowing it with therapeutic properties, including anti-inflammatory and antimicrobial effects [14].

The functionalization of starch/PVA-based scaffolds with CuO NPs synthesized from T. ornata extract offers a novel strategy to develop advanced biomaterials with dual physicochemical and biological functionalities [15]. These composite nanoscaffolds are envisioned to support tissue regeneration while concurrently mitigating inflammation, which is a critical factor in various pathological conditions, including chronic wounds, arthritis, and inflammatory skin disorders [16]. Inflammatory responses, if left unchecked, can impede tissue healing and lead to fibrosis or chronic diseases. Thus, designing biomaterials with intrinsic anti-inflammatory properties is essential for promoting favorable clinical outcomes [17]. In this light, evaluating the anti-inflammatory potential of the developed nanoscaffolds through in vitro assays—such as protein denaturation inhibition and xanthine oxidase inhibition—can offer insights into their biomedical applicability [18].

Moreover, comprehensive physicochemical characterization of the synthesized nanoparticles and scaffolds is vital to establish their structural, optical, thermal, and morphological attributes [19]. Techniques such as UV–visible spectroscopy, Fourier-transform infrared (FTIR) spectroscopy, X-ray diffraction (XRD), scanning electron microscopy (SEM), thermogravimetric analysis (TGA), and dynamic light scattering (DLS) are indispensable in confirming nanoparticle formation, understanding interaction between scaffold components, and assessing stability and surface charge. Such characterization not only ensures reproducibility and reliability of the synthesized materials but also provides essential information for tailoring scaffold properties to meet specific biomedical requirements [20].

The novelty of the present study lies in the integration of marine-derived CuO NPs into a biodegradable polymeric matrix using a sustainable and cost-effective approach [21]. Unlike conventional strategies that rely solely on synthetic materials and harsh fabrication processes, this research capitalizes on the natural bioactivity of T. ornata and the eco-friendly synthesis of therapeutic nanoparticles [22]. Furthermore, by combining these bioactive nanoparticles with starch/PVA nanofibers via electrospinning [23], the study endeavors to produce nanoscaffolds that not only support structural regeneration but also offer biological protection against inflammation—an aspect crucial for promoting effective tissue healing [24].

To the best of knowledge, this is among the first comprehensive reports exploring the fabrication of starch/PVA-based electrospun scaffolds incorporating CuO NPs synthesized using T. ornata extract, with a focus on both physicochemical and anti-inflammatory evaluation. Through this integrative approach, the study aims to demonstrate the feasibility of using marine algal resources for developing next-generation biomedical materials that combine structural support, bioactivity, and environmental sustainability.

2. Materials and methods

2.1. Chemicals and reagents

The present study employed T. ornata seaweed collected from the coastal belt of Rameswaram, Tamil Nadu, India, to facilitate the green synthesis of CuO NPs. Copper (II) sulfate pentahydrate ($CuSO_4 \cdot 5H_2O$), sourced from Sigma-Aldrich, was utilized as the metal precursor. PVA, with an approximate molecular weight of 115,000, served as the primary polymer matrix for electrospinning. Starch, obtained from a local supplier, was included to enhance the scaffold's structural features. All other chemicals and solvents, such as ethanol and Milli-Q water, were of analytical grade and purchased from Merck and Sigma-Aldrich. Electrospinning was performed using the HOLMARC HO-NFES-040 unit equipped with a precision syringe pump. Analytical characterization involved various instruments, including a VIS SPEC V-730 UV–Visible spectrophotometer, PerkinElmer Spectrum Two FTIR spectrometer, Bruker D8 Advance X-ray diffractometer, JEOL JSM-IT800 NANO SEM, Malvern Zetasizer Ultra for DLS and zeta potential analysis, and PerkinElmer TGA 8000 for thermal stability evaluation.

2.2. Collection and processing of marine algae

Fresh specimens of T. ornata were hand-harvested from the coastal waters near Rameswaram. The collected T. Ornata was taxonomically identified and authenticated by Dr V. Veeragurunathan, CSIR-CSMCRI-Marine Algal Research Station, Mandapam Camp 623519, Tamil Nadu, India. A voucher specimen was prepared and deposited at the Herbarium of the CSIR-CSMCRI-Marine Algal Research Station, under the accession number: SI–2025–RMM–022. This authentication ensures botanical accuracy and standardization of the study material. The algae were first cleansed thoroughly under running tap water to remove extraneous particles, followed by multiple washes with distilled water to eliminate any residual salt and contaminants. Approximately 100 grams of cleaned samples were chopped and air-dried at ambient room temperature over two weeks. Once fully dehydrated, the material was finely powdered using a mechanical grinder and stored in airtight containers for further processing.

2.3. Extraction via ultrasonic treatment

To extract bioactive compounds, 2 grams of powdered T. ornata were added to 50 mL of Milli-Q water in a sterile 100 mL beaker. The suspension was subjected to ultrasonic-assisted extraction at 60°C for 45 minutes using a LABQUEST ultrasonic cleaner (Borosil; Serial No. 941032329018). Post-sonication, the extract was filtered through Whatman No. 1 filter paper under aseptic conditions. The resulting clear filtrate was stored at 10°C. For prolonged storage and future applications, the extract was lyophilized into a stable powdered form [25, 26].

2.4. Green synthesis of CuO NPs

Eco-friendly synthesis of CuO NPs was achieved by mixing 50 mL of 0.1 M $CuSO_4 \cdot 5H_2O$ solution with 10 mL of T. ornata extract (10 mg dissolved in 10 mL of Milli-Q water) in a 5:1 ratio. The reaction mixture was stirred at 650 rpm and maintained at 60°C for two hours. A visible color shift from blue to bluish-green confirmed nanoparticle formation. The product was centrifuged and washed three times with double-distilled water to remove impurities. The cleaned nanoparticles were freeze-dried over 48 hours, resulting in a fine powder used for subsequent studies [27].

2.5. Electrospinning of starch/PVA scaffolds loaded with CuO NPs

A 15% (w/w) aqueous solution of fully hydrolyzed PVA was prepared by dissolving the polymer with continuous stirring at elevated temperatures. To this solution, 100 mg each of starch and synthesized CuO NPs were added, followed by stirring at 50°C for 2.5 hours to ensure uniform dispersion. The mixture was transferred into a syringe fitted with a 0.84 mm internal diameter needle and electrospun using a HOLMARC HO-NFES-040 system powered by a HMPSKV30 unit (0–30 kV, 0.5 mA). Optimal electrospinning conditions included a voltage of 11.5 kV, 12.3 cm distance from needle to collector, and a feed rate of 0.4 mL/h. Electrospinning was carried out at room temperature for 6–8 hours to yield nanofibrous mats [12, 13, 28].

2.6. Physicochemical characterization

2.6.1. UV–visible spectroscopy

UV–Visible spectral analysis was performed using a VIS SPEC V-730 spectrophotometer to confirm nanoparticle formation and assess optical properties. Spectral data were recorded for T. ornata extract, CuO NPs, and starch/PVA/CuO scaffolds over the 200–800 nm range using deionized water as a blank. Detection of surface plasmon resonance (SPR) peaks confirmed the presence and integration of nanoparticles [29].

2.6.2. FTIR spectroscopy analysis

FTIR spectra were recorded with a PerkinElmer Spectrum Two spectrometer in ATR mode, ranging from 4000 to 400 cm^{-1} with 64 scans at a 4 cm^{-1} resolution. This technique identified functional groups and molecular interactions within T. ornata extract, CuO NPs, and composite nanofibers. Characteristic bands representing –OH, C=O, amide, and Cu–O groups confirmed successful nanoparticle incorporation [30].

2.6.3. XRD analysis

The crystalline structure of CuO NPs and nanofiber composites was examined using a Bruker D8 Advance diffractometer with CuKα radiation ($\lambda = 1.5406$ Å) at 40 kV and 40 mA. Scanning was performed from 5° to 90° (2θ) with a step size of 0.029649°. The diffractograms revealed distinct peaks confirming the monoclinic phase of CuO and its incorporation into the polymer matrix [31].

2.6.4. SEM analysis

SEM was conducted using a JEOL JSM-IT800 NANO SEM to observe surface morphology and nanoparticle distribution in scaffolds. Samples were gold-coated to enhance conductivity before imaging. SEM micrographs illustrated surface texture, nanoparticle dispersion, and fiber uniformity [32].

2.6.5. TGA

Thermal behavior of the composite scaffolds was assessed with a PerkinElmer TGA 8000 system. About 5 mg of each sample was heated from room temperature to 550°C at a rate of 15°C/min under nitrogen atmosphere. Thermograms provided data on moisture evaporation, decomposition patterns, and overall thermal resistance [33].

2.6.6. Particle size and zeta potential

DLS and zeta potential analyses were conducted using a Malvern Zetasizer Ultra. DLS determined nanoparticle size distribution, while zeta potential values indicated the surface charge and stability of colloidal suspensions. Higher absolute values denoted excellent suspension stability, essential for biomedical uses [34].

All raw data have been archived in the Mendeley Data repository (DOI: 10.17632/tgxw2g4stx.1) for transparency and accessibility.

2.7. Anti-inflammatory assays

2.7.1. Protein denaturation inhibition assay

The anti-inflammatory efficacy of the samples was assessed using a modified version of the heat-induced protein denaturation assay. Each test mixture consisted of 0.45 mL of 5% aqueous bovine serum albumin and 0.05 mL of test sample (algal extract, CuO NPs, starch/PVA/CuO scaffolds, or diclofenac sodium). Sample concentrations were 25, 50, 75, and 100 µg/mL. The pH was adjusted to 6.3 with 1 N HCl, followed by incubation at 37°C for 20 minutes. Subsequently, the tubes were heated at 57°C for 3 minutes and cooled to room temperature. Turbidity due to protein denaturation was measured at 660 nm spectrophotometrically [35].

2.7.2. Xanthine oxidase inhibition assay

Xanthine oxidase inhibitory activity was evaluated following a slightly modified standard protocol. The reaction mixture included 0.3 mL of each sample (algal extract, CuO NPs, starch/PVA/CuO scaffolds, or diclofenac sodium) at varying concentrations (25, 50, 75, and 100 µg/mL), 0.5 mL of 0.15 mM xanthine solution (prepared in phosphate buffer, pH 7.5), and 0.2 mL of xanthine oxidase enzyme (0.1 units/mL). After 15 minutes of incubation at 25°C, the absorbance was recorded at 295 nm. A blank lacking the enzyme was used as control [36].

2.8. Statistical analysis

Experimental data were evaluated using SPSS v25.0 and GraphPad Prism v9.0. All assays were performed in triplicate, and results were expressed as mean ± standard deviation. One-way ANOVA followed by Tukey's or Dunnett's post-hoc tests was used to assess statistical significance ($p < 0.05$). Data normality was examined using the Shapiro–Wilk test. Where necessary, logarithmic transformation was applied. Pearson's correlation coefficient was calculated to analyze relationships between variables. All conclusions were drawn with a 95% confidence level for precision and reliability [37].

3. RESULTS

3.1 UV–visible spectroscopy

The UV–Vis analysis (Figure 1) demonstrated distinct optical signatures for both the T. ornata extract and the biosynthesized CuO NPs. The algal extract showed a broad absorption profile within 200–400 nm, with a pronounced peak at approximately 346 nm (absorbance value: 1.943), indicative of phytoconstituents such as phenolics, flavonoids, and chlorophyll derivatives. In contrast, the CuO NPs exhibited a sharp absorbance peak near 200 nm, suggestive of surface plasmon resonance typical of nanoscale entities. The clearly differentiated spectral responses between the extract and the nanoparticles affirm the successful biosynthesis and the active role of biomolecules in reduction and stabilization. The presence of these nanoparticles in nanofiber matrices underscores their prospective use in UV filtration and photocatalytic applications.

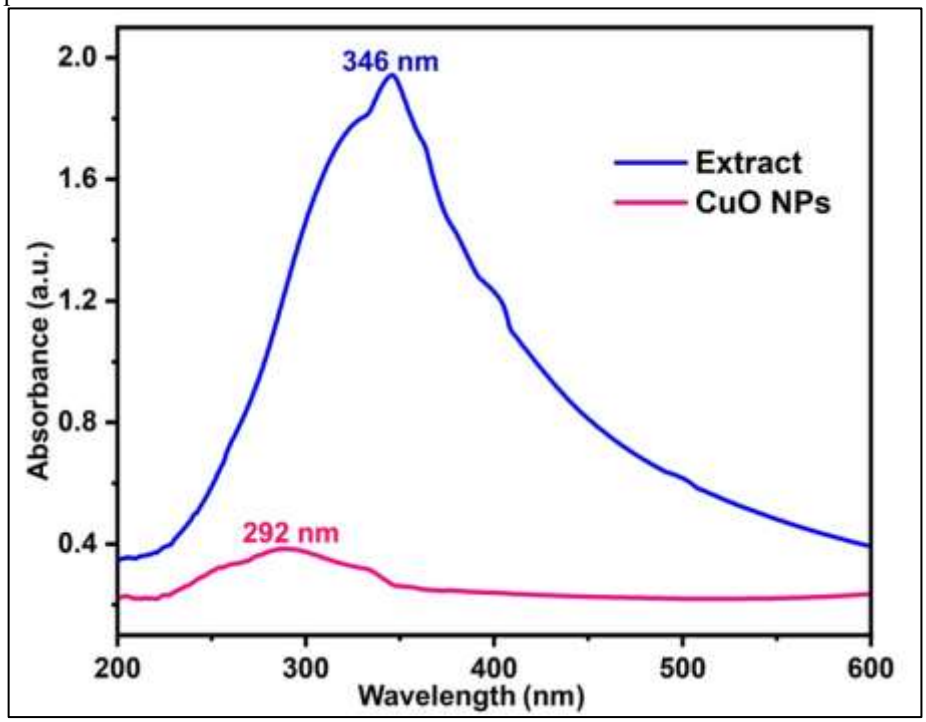

Figure 1. UV–Visible spectral profiles of algal extract and CuO NPs.

3.2 FTIR analysis

FTIR spectral analysis (Figure 2) validated the chemical signatures of CuO NPs and the engineered nanofibrous matrices. The CuO NPs presented characteristic bands at 601 cm^{-1} (Cu–O vibrational stretch), 863 cm^{-1} (metal–oxygen linkages), and 1061 cm^{-1} (C–O stretching), along with a broad absorption at 3122 cm^{-1}, corresponding to hydroxyl groups—likely from residual moisture or capping phytochemicals. In the nanoscaffold spectra, prominent peaks appeared at 3284 cm^{-1} (O–H/N–H stretches), 2921 cm^{-1} (C–H stretching), and 1710 cm^{-1} (C=O groups), revealing the presence of the starch/PVA polymer matrix. Additional signals at 1328 cm^{-1} and 1087 cm^{-1} indicated glycosidic and amine functionalities. The persistence of Cu–O related bands alongside polymeric features confirmed effective nanoparticle embedding with no major chemical interference.

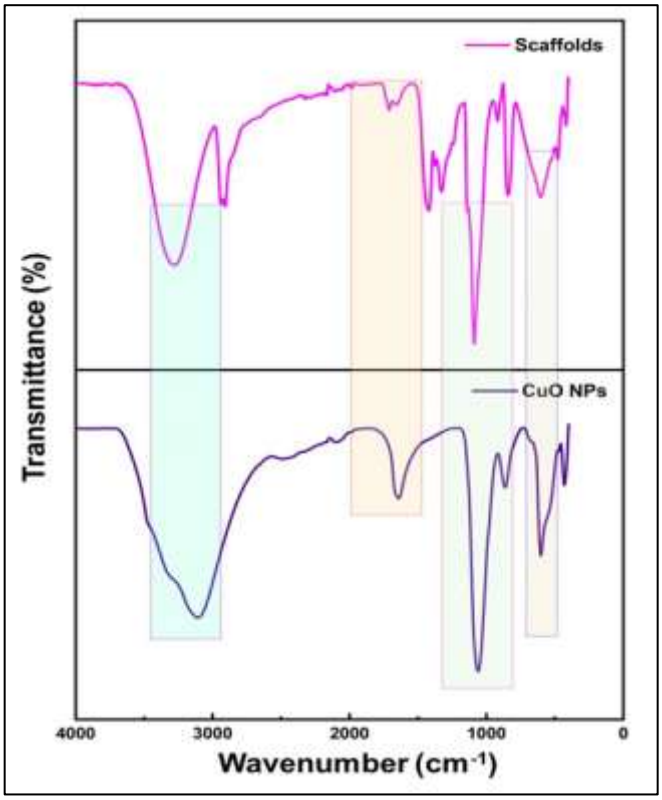

Figure 2. FTIR spectra of CuO NPs and their incorporation into nanoscaffolds

3.3 XRD analysis

XRD profiles (Figure 3) confirmed the crystalline structure of CuO NPs and their distribution within the nanoscaffolds. CuO NPs displayed 28 sharp diffraction peaks in the 2θ range of 5°–90°, with significant reflections at 24.435°, 32.876°, and 38.504°, aligning with monoclinic CuO per JCPDS file No. 48-1548. The nanoscaffolds exhibited broader, less intense peaks—most notably at 21.420°, 29.372°, and 57.572°—indicating a semi-crystalline structure with an estimated 17.4% crystallinity. The broadened peaks and slight angular shifts suggest reduced crystalline order due to polymer incorporation and confirm successful nanoparticle integration within the scaffold matrix.

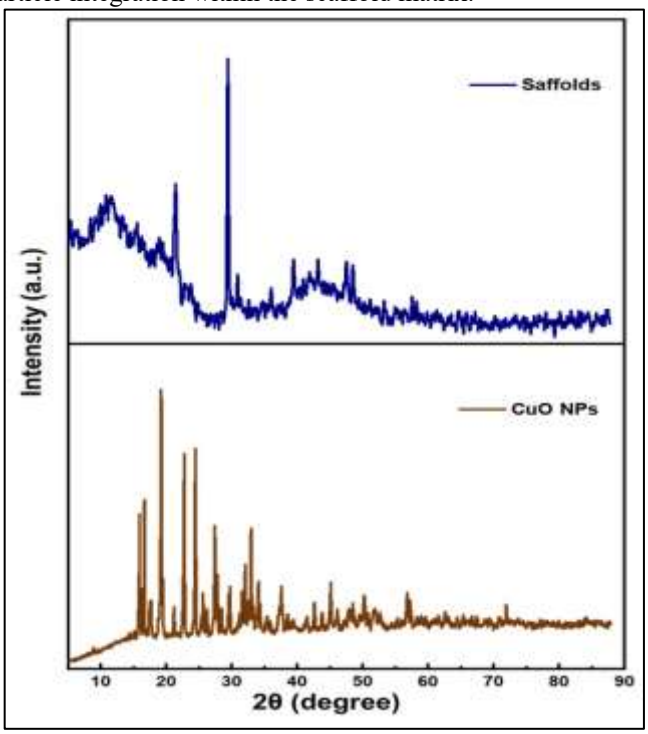

Figure 3. XRD patterns of synthesized CuO NPs and CuO-loaded scaffolds

3.4 SEM analysis

SEM (Figure 4) revealed that the CuO NPs were mostly spherical to irregular in shape, ranging from 90 to 100 nm in size, with minor aggregation likely caused by surface energy. The electrospun starch/PVA nanofibers appeared uniform, smooth, and free of beads, with diameters between 150 and 300 nm. Embedded nanoparticles were observed along the

fiber surface, exhibiting generally uniform dispersion with minimal agglomeration. Occasionally, larger NP clusters were noticed, probably due to interfacial interactions. The fibers formed a consistent porous network structure favorable for biomedical applications. These results confirm effective nanoparticle formation and incorporation, although further improvements in NP dispersion are feasible.

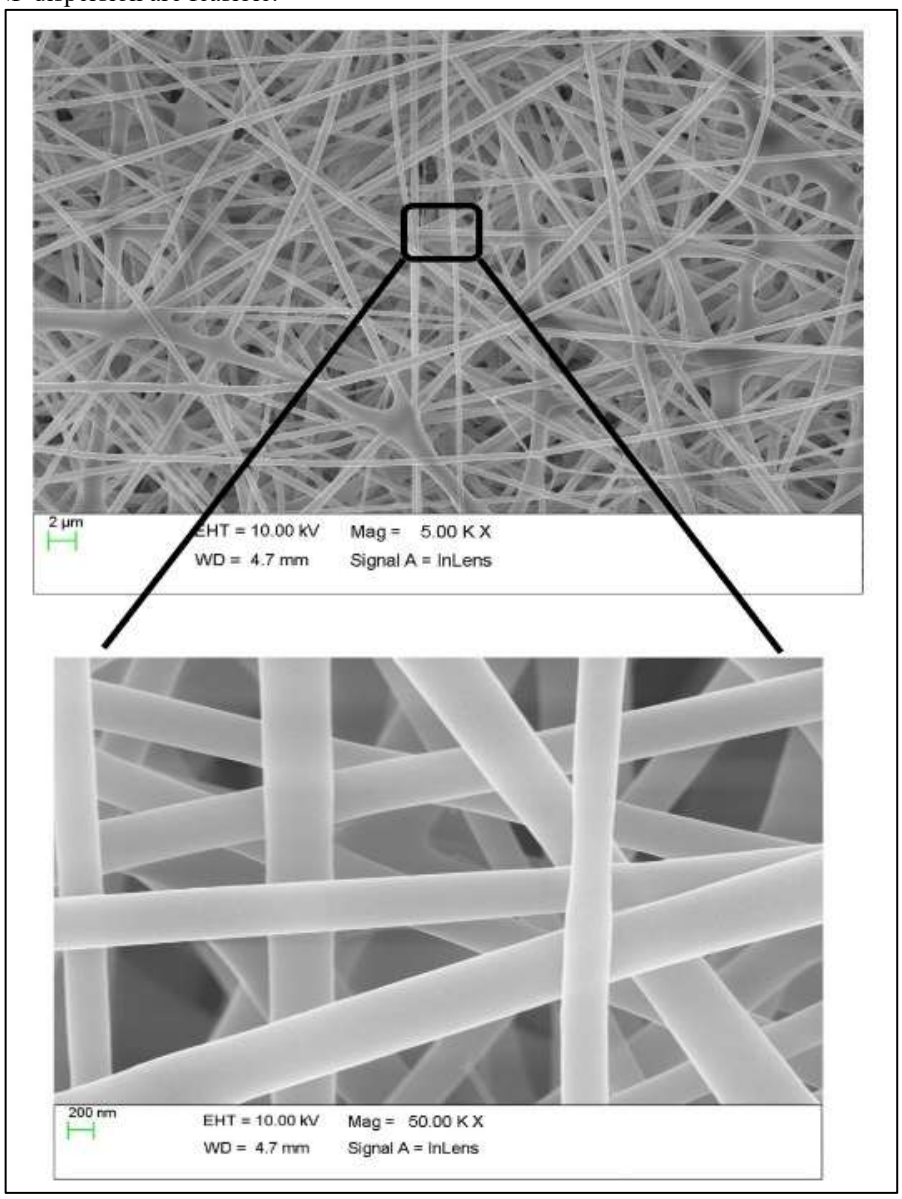

Figure 4. SEM analysis of starch/PVA/CuO-NPs nanoscaffolds

3.5 TGA

TGA (Figure 5) assessed the thermal behavior of nanoscaffolds containing CuO NPs. A 2.315 mg sample was subjected to heating from 30°C to 550°C at a rate of 15°C/min under a nitrogen atmosphere. Initial mass loss of 9.509% occurred due to evaporation of water and volatile components. Significant degradation commenced at 244.81°C, peaked at 332.83°C, and ended at 378.85°C, associated with decomposition of the starch/PVA matrix. A total weight reduction of 41.696% was recorded by 550°C. The presence of CuO NPs appeared to enhance the thermal stability of the scaffold, as indicated by delayed onset of degradation and higher residual mass compared to the unmodified polymer matrix.

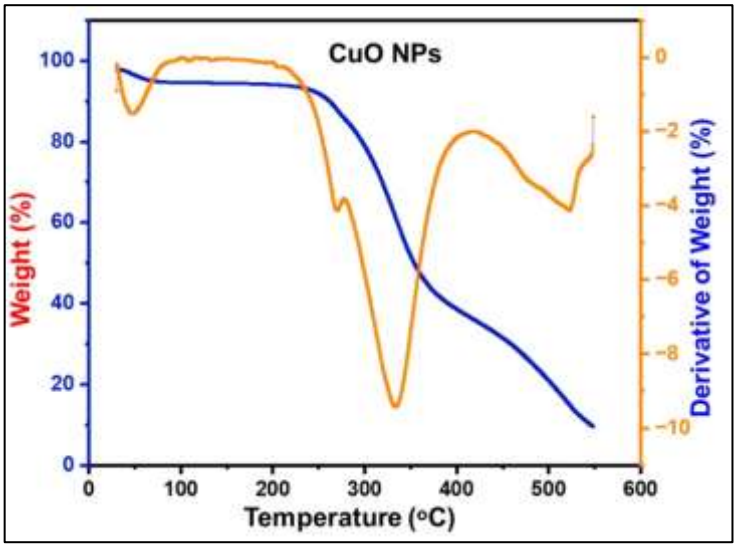

Figure 5. Thermal degradation behavior of CuO-incorporated nanoscaffolds.

3.6 Zeta potential and particle size distribution

DLS measurements revealed a bimodal particle size distribution for the CuO NPs, with an average hydrodynamic diameter of 92.8 nm (Figure 6) and a polydispersity index (PDI) of 0.5592, suggesting moderate size variation. The recorded count rate was 3465 kcps, indicating a relatively stable dispersion during analysis. The zeta potential value measured at -5.29 mV (Figure 7) reflected weak electrostatic repulsion and limited colloidal stability. This low surface charge favors aggregation, consistent with SEM results. These observations point to the need for surface functionalization strategies to enhance colloidal stability and prevent aggregation in prolonged biological or environmental exposures.

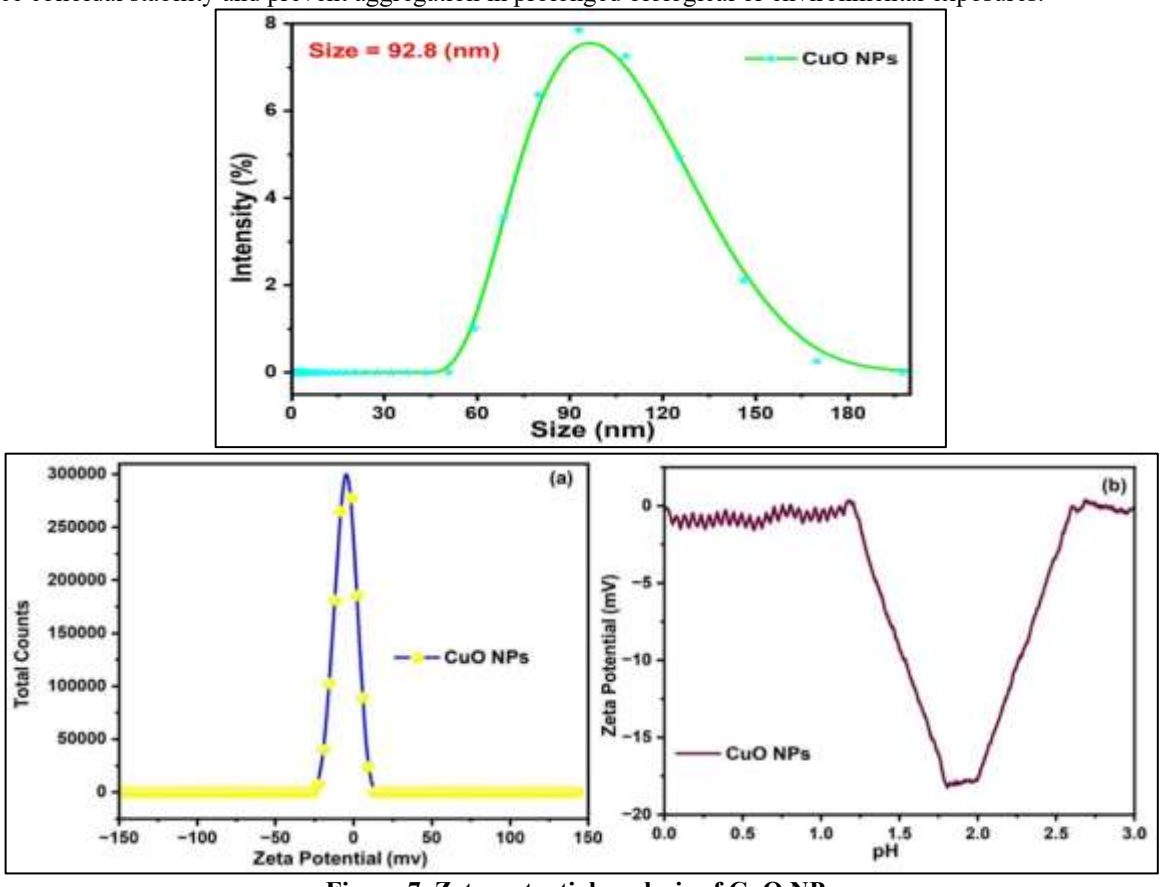

Figure 7. Zeta-potential analysis of CuO NPs

3.7. Anti-inflammatory assays

3.7.1. Protein denaturation inhibition assay

The anti-inflammatory potential of algal extract, CuO NPs, and starch/PVA/CuO-NPs nanoscaffolds was evaluated through their ability to inhibit heat-induced protein denaturation (Figure 8). The results demonstrated concentration-dependent inhibition across all tested samples. At the lowest concentration (25 µg/mL), the algal extract exhibited an inhibition of 19.01%, while CuO NPs and nanoscaffolds showed 23.01% and 26.01% inhibition, respectively. As the concentration increased to 50 µg/mL, the inhibition rates rose to 34.42% (extract), 38.42% (CuO NPs),

and 40.42% (nanoscaffolds). Further enhancement was observed at 75 µg/mL, with values reaching 53.54%, 58.54%, and 62.54% for the extract, CuO NPs, and nanoscaffolds, respectively. At the highest concentration (100 µg/mL), the nanoscaffolds displayed the strongest inhibition (79.21%), outperforming CuO NPs (69.21%) and the algal extract (63.21%). These results suggest that the nanoscaffolds possess superior anti-inflammatory activity, likely due to the synergistic effects of starch/PVA and CuO NPs.

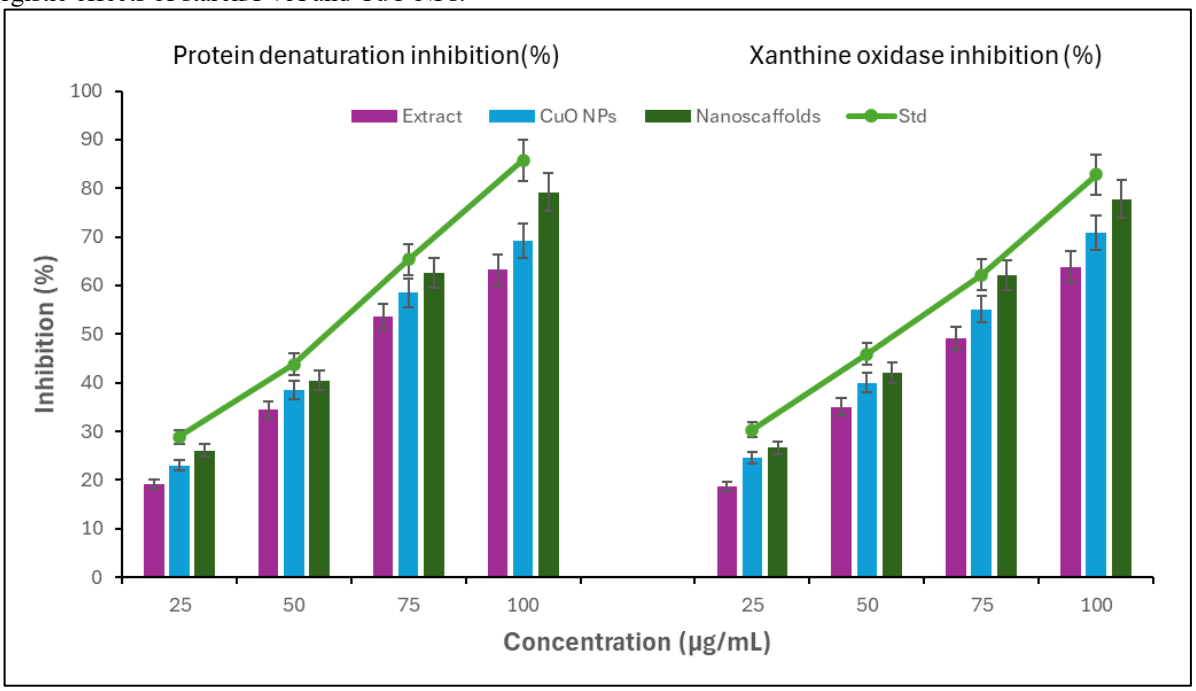

Figure 8. Anti-inflammatory activity analysis of algal extract, CuNPs and starch/PVA/CuONPs nanoscaffolds

A second set of experiments under modified conditions yielded consistent trends. At 25 µg/mL, the extract, CuO NPs, and nanoscaffolds inhibited denaturation by 18.61%, 24.61%, and 26.61%, respectively. The inhibition increased progressively with concentration, culminating at 100 µg/mL with values of 63.81% (extract), 70.81% (CuO NPs), and 77.81% (nanoscaffolds). The nanoscaffolds again exhibited the highest efficacy, reinforcing their potential as an anti-inflammatory agent.

3.7.2. Xanthine oxidase inhibition assay

The xanthine oxidase inhibition assay (Figure 8) further validated the anti-inflammatory properties of the samples. Similar to the protein denaturation assay, the inhibition was concentration-dependent. At 25 µg/mL, the algal extract, CuO NPs, and nanoscaffolds demonstrated inhibition rates of 19.01%, 23.01%, and 26.01%, respectively. By 50 µg/mL, these values increased to 34.42%, 38.42%, and 40.42%, indicating enhanced activity at higher doses. The trend continued at 75 µg/mL, with the nanoscaffolds achieving 62.54% inhibition, surpassing CuO NPs (58.54%) and the extract (53.54%). At 100 µg/mL, the nanoscaffolds again led with 79.21% inhibition, followed by CuO NPs (69.21%) and the extract (63.21%).

In the replicate experiment, the results aligned closely, with the nanoscaffolds consistently outperforming the other samples. For instance, at 100 µg/mL, they exhibited 77.81% inhibition, compared to 70.81% for CuO NPs and 63.81% for the extract. This assay highlights the nanoscaffolds' ability to suppress xanthine oxidase activity, a key enzyme in inflammatory pathways, further supporting their anti-inflammatory efficacy.

Both assays confirmed that the starch/PVA/CuO-NPs nanoscaffolds exhibit the highest anti-inflammatory activity among the tested samples, followed by CuO NPs and the algal extract. The nanoscaffolds' superior performance may be attributed to the combined effects of their components, which enhance bioavailability and interaction with inflammatory markers. These findings suggest promising applications for nanoscaffolds in anti-inflammatory therapies, warranting further in vivo studies.

4. DISCUSSION

The biosynthesis of CuO NPs using T. ornata extract and their integration into starch/PVA nanofibrous scaffolds were successfully validated through a comprehensive set of characterization techniques and bioactivity assays. Each analytical method provided crucial insight into the physicochemical and biological properties of the synthesized nanomaterials, collectively supporting their potential for biomedical applications, particularly in anti-inflammatory therapies [38-42].

The UV–Visible spectroscopy results revealed distinct absorption profiles for the algal extract and the synthesized CuO NPs [43, 44]. The extract exhibited a broad absorbance band from 200 to 400 nm with a strong peak at 346 nm, suggesting the presence of bioactive phytocompounds like flavonoids, phenolics, and chlorophyll derivatives. These constituents likely played a critical role in reducing and stabilizing the metal ions during nanoparticle formation. Conversely, the CuO NPs displayed a sharp peak near 200 nm, characteristic of surface plasmon resonance in metal nanoparticles [45-48]. The differences between the spectra of the extract and the nanoparticles serve as evidence of nanoparticle synthesis, with the presence of phytochemicals serving dual functions as reducing and capping agents [49, 50]. These results also underscore the potential of CuO NPs for UV protection and photocatalytic activity [51-54].

FTIR spectroscopy further confirmed the presence of functional groups related to both the CuO NPs and the polymer scaffold. In the CuO NPs, characteristic bands at 601 cm^{-1} and 863 cm^{-1} corresponded to Cu–O vibrations and metal–oxygen linkages, while a broad absorption at 3122 cm^{-1} indicated hydroxyl groups—likely from residual phytochemicals used in the synthesis process. The nanoscaffolds exhibited peaks at 3284 cm^{-1} (O–H/N–H stretching), 2921 cm^{-1} (C–H stretching), and 1710 cm^{-1} (C=O stretching), confirming the incorporation of starch/PVA. Importantly, the continued presence of Cu–O signals within the scaffold spectrum indicated that nanoparticle embedding did not disrupt the structural integrity of either component. This validates the efficient incorporation of CuO NPs into the polymer matrix without adverse chemical interactions [55-59].

XRD analysis provided structural confirmation of the crystalline nature of the synthesized CuO NPs and the semi-crystalline nature of the nanoscaffolds [60, 61]. The CuO NPs exhibited sharp diffraction peaks corresponding to a monoclinic crystalline structure, aligning with JCPDS file No. 48-1548 [62, 63]. In contrast, the nanoscaffolds displayed broader peaks, reflecting their semi-crystalline composition due to the starch/PVA matrix. The slight peak broadening and reduced crystallinity (~17.4%) in the scaffolds imply that the integration of the nanoparticles affected the crystalline order, likely due to polymer interference. This reduced crystallinity may enhance the mechanical flexibility and drug release properties of the nanofibers, making them suitable for biomedical uses [64-69].

SEM highlighted the morphological characteristics of both the CuO NPs and the composite nanofibers [70]. The CuO NPs appeared as spherical to irregularly shaped entities with sizes ranging from 90 to 100 nm. Slight aggregation was observed, potentially due to the high surface energy and weak electrostatic repulsion. The starch/PVA nanofibers were smooth and bead-free, with uniform diameters between 150 and 300 nm. Nanoparticles were visibly embedded on the fiber surfaces, with a generally homogeneous distribution. Occasional clustering of nanoparticles suggests room for optimization, particularly in improving dispersion techniques to minimize agglomeration. Nonetheless, the porous, interconnected fiber network supports the use of these materials in tissue engineering and drug delivery [71, 72].

TGA illustrated the thermal behavior of the nanoscaffolds. The presence of CuO NPs contributed to improved thermal stability, evidenced by a delayed onset of degradation and a reduced total weight loss. The initial weight loss (~9.5%) up to 100°C was attributed to the evaporation of moisture and volatile compounds. Major thermal decomposition occurred between 244.81°C and 378.85°C, corresponding to the degradation of the polymer matrix. The final residual mass at 550°C was greater in the nanocomposite scaffold than in the pure polymer, confirming the thermal reinforcement effect of the nanoparticles [73].

DLS and zeta potential measurements assessed the colloidal properties of the synthesized CuO NPs [74]. The average particle size was 92.8 nm with a polydispersity index of 0.5592, indicating moderate size uniformity. The low zeta potential of -5.29 mV suggested limited electrostatic stability, explaining the nanoparticle aggregation observed in SEM images. This low surface charge might reduce colloidal stability over time, indicating the need for surface modifications or the addition of stabilizing agents to enhance dispersibility in biological systems [75].

The anti-inflammatory potential of the synthesized materials was evaluated using protein denaturation and xanthine oxidase inhibition assays [76]. In both tests, the nanoscaffolds consistently exhibited the highest inhibitory activity, followed by CuO NPs and the algal extract. The protein denaturation assay revealed concentration-dependent inhibition, with the nanoscaffolds achieving a maximum of 79.21% inhibition at 100 µg/mL. These results were corroborated by a second set of experiments under modified conditions, reinforcing their reproducibility [77]. Similarly, the xanthine oxidase inhibition assay demonstrated strong inhibitory activity for the nanoscaffolds (up to 79.21%), suggesting effective suppression of this key inflammatory enzyme. The superior performance of the nanoscaffolds may be attributed to the synergistic interactions among the CuO NPs, the bioactive phytochemicals, and the starch/PVA matrix, which likely enhanced the bioavailability and targeted activity of the composite material [78].

The integration of biosynthesized CuO NPs into starch/PVA nanofibers was successfully achieved and confirmed through multiple characterization techniques. The resulting nanoscaffolds demonstrated favorable physicochemical properties, including appropriate size, structure, and stability, along with notable anti-inflammatory activity. These findings highlight their promise as potential candidates for biomedical applications, particularly in anti-inflammatory therapies. Future in vivo investigations will be critical to validate these outcomes and to assess long-term safety and efficacy.

5. CONCLUSION

This research successfully demonstrated the green synthesis of CuO NPs using T. ornata extract and their effective integration into starch/PVA-based nanofibrous scaffolds. Comprehensive characterization through UV–Vis, FTIR, XRD, SEM, TGA, and DLS analyses confirmed the formation, chemical stability, and uniform dispersion of CuO NPs within the polymer matrix. The resulting nanoscaffolds exhibited enhanced thermal stability, a well-defined porous morphology, and effective nanoparticle embedding without significant agglomeration. Moreover, anti-inflammatory assays revealed that the nanoscaffolds exhibited superior inhibition activity in both protein denaturation and xanthine oxidase assays compared to the algal extract and CuO NPs alone. This enhanced efficacy likely stems from the synergistic interaction between the bioactive components and the polymeric matrix, facilitating better bioactivity and stability. Overall, the study underscores the potential of starch/PVA/CuO-NP nanoscaffolds as multifunctional biomaterials for anti-inflammatory applications, paving the way for future investigations into their biomedical relevance in wound healing and drug delivery systems.

Ethical Declaration: Not applicable for this study.

Funding: Not available for this study.

Conflicts of Interest: The authors declare no conflicts of interest.

Data Availability Statement: The full dataset of physiochemical characterization associated with this work is published in Mendeley Data [Dataset] Eco-friendly nanocomposite scaffolds: physicochemical analysis of starch matrices integrated with Turbinaria ornata-mediated CuO nanoparticles (DOI: 10.17632/tgxw2g4stx.1). Disclosure: The material characterization data and figures (e.g., UV, SEM, FTIR, XRD, TGA, Zeta Potential and particle sizer) presented here were generated from a common dataset and are being reused across multiple related studies on nanomaterials. All biological analyses and conclusions are original to each manuscript.

REFERENCES

1. Natarajan PM. Dental Bioinformnatics-Current Scope and Future perspectives. Research Journal of Pharmacy and Technology. 2022;15(5):2351-6.
2. Vidhyarekha U, Natarajan PM, Bhuminathan S, Sabarinathan J, Suba R, Vijayalakshmi P. Role of artificial intelligence in Oral Cancer. Advances in Public Health. 2024. 2024: 3664408.
3. Ganesan A, Kumar NG, Natarajan PM, Gauthaman J. Automated classification of elongated styloid processes using deep learning models-an artificial intelligence diagnostics. Frontiers in Oral Health. 2025; 5: 1424840.
4. Umapathy VR, Natarajan PM, Swamikannu B. Regenerative Strategies in Dentistry: Harnessing Stem Cells, Biomaterials and Bioactive Materials for Tissue Repair. Biomolecules. 2025; 15: 546.
5. Natarajan PM, Umapathy VR, Murali A, Swamikannu B. (2022). Computational Simulations of Identified marine-derived Natural Bioactive Compounds As Potential Inhibitors of Oral Cancer. Future Science OA. 2022; 8(3).
6. Surendran N, Chandrasekaran G, Raju MV, Chandrasekaran MK, Ahalliya RM, Palanisamy CP, Kanniappan GV, Arcot R, Alharbi NS, Thiruvengadam M. Anti-inflammatory potential of ethanolic extract of Maranta arundinacea L.: Insights from COX-2 modulation and oxidative stress analysis. South African Journal of Botany. 2026; 195: 142-151.
7. Pei J, Senthilkumar MV, Hessini K, Subramaniyam S, Sivaramakrishnan R, Kanniappan GV, Jayaraman S, Palanisamy CP. Green fabrication of starch/PVA/CuO nanoscaffolds using marine macroalgae extract for enhanced anti-inflammatory activity. Sustainable Chemistry and Pharmacy. 2026; 51: 102397.
8. Balasubramanian V, Loganathan L, Muthuswamy K, Viswanathan TM, Raju MV, Chandrasekaran MK, Ahalliya RM, Poorasamy J, Palanisamy CP, Dominic S, Kanniappan GV. Anticancer therapeutic efficacy of PEGylated β-galactosidase from Aspergillus terreus in DMBA-induced breast cancer: Toxicological, molecular and histopathological evaluation in Wistar rats. International Journal of Biological Macromolecules. 2026; 360: 151856.
9. Jayaraman S, Eswaran A, Rajagopal P, Palanisamy CP, Veerakumar P, Veeraraghavan VP, Sirasanagandla SR. Neuroendocrine-associated epigenetic factors in cellular senescence: mechanisms and therapeutic implications. Biogerontology. 2026; 27(2): 64.
10. Ponnusamy B, Rajagopal P, Palanisamy CP, Veeraraghavan VP, Jayaraman S. Mechanistic Exploration of the anticancer activity of Justicia adhatoda Plant Leaf Ethanolic Extract against Colon Cancer Cells: An in silico and in vitro Approach. Asian Pacific Journal of Cancer Prevention. 2026; 27(3): 1069-1080.
11. Pei J, Saran VS, Sivaramakrishnan R, Kanniappan GV, Pandurangan V, Jayaraman S, Dhayalan VK, Mironescu M, Mironescu ID, Palanisamy CP. Ultrasonic-assisted, Sargassum ilicifolium (brown marine macroalgae)-mediated biogenic synthesis of CuO nanoparticles incorporated in starch/PVA electrospun nanoscaffolds: In vitro safety and antioxidant efficacy assessment. Bioorganic Chemistry. 2026; 173: 109679.
12. Raj MAPA, Subramaniyam S, Kanniappan GV, Jayaraman S, Palanisamy CP. Sustainable fabrication of starch/PVA/CuO electrospun nanoscaffolds from Turbinaria ornata (marine macroalgae) extract: Physicochemical characterization and antidiabetic evaluation. Kuwait Journal of Science. 2026; 53(2): 100545.
13. Pei J, Ganesh NS, Subramaniyam S, Sivaramakrishnan R, Kanniappan GV, Jayaraman S, Palanisamy CP. Sustainable fabrication of starch/PVA/CuO electrospun nanoscaffolds from Padina tetrastromatica (Brown macroalgae) extract: Physicochemical characterization and antidiabetic assessment. Sustainable Chemistry One World. 2026; 9: 100195.
14. Sakthiraj A, Sivaramakrishnan R, Subramaniyam S, Kanniappan GV, Pandurangan V, Jayaraman S, Dhayalan VK, Mironescu M, Mironescu ID, Palanisamy CP. Chemical Physics Impact. Starch/PVA electrospun nanoscaffolds loaded with ultrasonic-assisted green-synthesis of CuO nanoparticles from marine macroalgae (Gracilaria corticata) extract: Cytotoxicity and antioxidant analysis. 2026; 12: 101018.
15. Raju M, Chandrasekaran MK, Loganathan L, Ahalliya RM, Mironescu M, Mironescu ID, Palanisamy CP, Kanniappan GV. Lipid remodeling and ferroptosis in phosphatidylcholine-mediated tumor–stroma crosstalk. Frontiers in Molecular Biosciences. 2026; 13: 1742305.
16. Kunamalla R, Panagal M, Palanisamy CP. Biogenic synthesis and fabrication of starch/PVA/CuO electrospun nanoscaffolds from Sargassum ilicifolium (brown marine macroalgae) extract for anticancer activity on HT-29 and MCF-7 cancer cells. Biocatalysis and Agricultural Biotechnology. 2026; 72: 103923.
17. Pei J, Govindaraj H, Sivaramakrishnan R, Kanniappan GV, Pandurangan V, Dhayalan VK, Mironescu M, Mironescu ID, Jayaraman S, Palanisamy PC. Sustainable fabrication of biopolymer-based (starch/PVA) nanoscaffolds loaded with green-synthesized CuO nanoparticles from Sargassum wightii (marine macroalgae): Cytocompatibility and antioxidant activity. Biomaterials Advances. 2026; 182: 214660.
18. Pei J, Perumal NC, Meng P, Long Q, Palanisamy CP. Extracellular vesicle-based biosensors for Alzheimer's disease: A new frontier in precision diagnostics. Ageing Research Reviews. 2026; 113: 102904.

19. Shree P, Sivaramakrishnan R, Kanniappan GV, Pandurangan V, Jayaraman S, Dhayalan VK, Mironescu M, Mironescu ID, Palanisamy CP. Antioxidant and biocompatible CuO-starch/PVA nanoscaffolds via ultrasonic green synthesis using Turbinaria conoides (brown marine macroalgae). Medicine in Drug Discovery. 2025; 28: 100238.
20. Gong J, Lin J, Guan T, Pei J, Palanisamy CP, El-AtyFrom AMA. selenium tolerance to nanoplastic antagonism: Comprehensive characterization of L. casei SNUT1 and its extracellular vesicle–nanoselenium complex. Food Bioscience. 2025; 74: 107749.
21. Poochi SP, Sundarraj R, Raju MV, Chandrasekaran MK, Ahalliya RM, Palanisamy CP, Kanniappan GV, Kondapavuluri BK, Thiruvengadam M. Harnessing Nature: Computational and Experimental Insights Into Ipomoea obscura Metabolites for Bladder Cancer Therapy. Chemistry and Biodiversity. 2025; 0: e00909.
22. Dugganaboyana GK, Kannankumar MKG, Shivaramakrishna S, Raju MV, Chandrasekaran MK, Ahalliya RM, Panneerselvam N, Palanisamy CP, Kanniappan GV. Phytochemical insights, antioxidant activity and therapeutic potential of Cassia senna against prostate cancer in Wistar albino rats. Discover Applied Sciences. 2025; 7:1206.
23. Natarajan SR, Krishnamoorthy R, Alshuniaber MA, Gatasheh MK, Rajagopal P, Veeraraghavan VP, Palanisamy CP, Jayaraman S. KDM1A Facilitates Oncogenic Potential in Colorectal Cancer Progression Through the Activation of AXIN/GSK3β/β-Catenin Signaling Pathways: Evidence From Integrated Transcriptomics and In Vitro Studies. The Journal of Gene Medicine. 2025; 27(11): e70053.
24. Guan T, Gong J, Lin J, Palanisamy CP, Jinjin Pei J, El-Aty AMA. Machine learning-driven multimodal optimization of selenium biotransformation and flavor profiling in fermented apple–Yacon functional beverages. Innovative Food Science & Emerging Technologies. 2025; 105: 104198.
25. Natarajan SR, Krishnamoorthy R, Alshuniaber MA, Alsulami TS, Gatasheh MK, Rajagopal P, Palanisamy CP, Govindan R, Veeraraghavan VP, Jayaraman S. ABCE1 facilitates tumour progression via aerobic glycolysis and inhibits cell death in human colorectal cancer cells through the p53 signalling pathway. Scientific Reports. 2025; 15: 24674.
26. Huang Y, Guo H, Liu Y, Jin W, Palanisamy CP, Pei J, Oz F, El-Aty AMA. Effects of Natural Polysaccharides on the Gut Microbiota Related to Human Metabolic Health. Molecular Nutrition & Food Research. 2025; 69:e202400792.
27. Poornima K, Meenakshi K.C, Manikandan V.R, Shankari G, Prabhu D, Rathi M.A, Palanisamy CP, Balaji R, Gopalakrishnan V.K. Exploring the anticancer potential of Jerantinine A from Tabernaemontana coronaria against prostate, breast, and ovarian cancers: A computational approach. Journal of Complementary and Integrative Medicine, 2025 22(2): 363–372.
28. Palanisamy CP, Poompradub S, Sansanaphongpricha K, Jayaraman S, Subramani K. Faridah Sonsudin gGreen synthesis of Nigella sativa-mediated silver nanoparticles for enhanced antibacterial activity and wound healing: Mechanistic insights and biomedical applications. Environmental Nanotechnology, Monitoring & Management. 2025; 24: 101085.
29. Surendran N, Raju MV, Chandrasekaran MK, Ahalliya RM, Palanisamy CP, Chandrasekaran G, Kanniappan GV. Physicochemical characterization of starch from Maranta arundinacea L.(arrowroot) rhizomes and its inhibition of COX-2: In vivo validation. Bioactive Carbohydrates and Dietary Fibre. 2025; 33: 100465.
30. Kannappan P, Chandrasekaran MK, Raju MV, Gopalakrishnan S, Dhamodharan P, Ahalliya RM, Palanisamy CP, Raju B, Kanniappan GV. Exploring the anticancer potential of Jerantinine A from Tabernaemontana coronaria against prostate, breast, and ovarian cancers: a computational approach. Journal of Complementary and Integrative Medicine. 2025; 22(02): 363-372.
31. Ganesan A, Kumar NG, Natarajan PM. Solanum trilobatum leaf extract-derived silver nanoparticles downregulate the PI3K/AKT/mTOR signaling pathway and attenuate oral squamous cell carcinoma cell proliferation. Journal of Herbmed Pharmacology. 2024; 13(2): 300-307.
32. Perumal MKK, Renuka RR, Subbiah SK, Natarajan PM. Artificial intelligence-driven clinical decision support systems for early detection and precision therapy in oral cancer: a mini review. Frontiers in Oral Health. 2025; 6: 1592428.
33. Ramesh E, Ganesan A, Lakshmi KC, Natarajan PM. Artificial intelligence-based diagnosis of oral leukoplakia using deep convolutional neural networks Xception and MobileNet-v2. Frontiers in Oral Health. 2025; 6: 1414524.
34. Natarajan PM. Computational Studies on Recent Congeners of Fluoroquinolones and Nitroimidazoles for Their Use in Periodontal Therapy. Journal of Pharmacy and Bioallied Sciences. 2024; 16(5): S4731-S4740.
35. Ganesan A, Kumar NG, Natarajan PM. Anticancer activity of silver nanoparticles synthesized from aqueous leaf extract of Solanum trilobatum (Purple fruit pea eggplant) on human oral cancer cells. Journal of Herbmed Pharmacololgy. 2024; 13(2): 260-268.
36. Umapathy V, Dhanavel A, Kesavan R, Natarajan PM, Bhuminathan S, Vijayalakshmi P. Anticancer Potential of the Principal Constituent of Piper nigrum, Piperine: A Comprehensive Review. Cureus. 2024; 16(2): e54425.
37. Natarajan PM, Bhuminathan S, Rajan R, Bindu K, Loganathan K, Veerakumar R. The Crucial Role of Smoking Cessation in Preventing Oral Cancer. Journal of Pharmacy and Bioallied Sciences. 2024; 16(5): S4245-S4247.
38. Umapathy VR, Swamikannu B, Natarajan PM, Devi R, Nandini MS, Vimalarani, Vijayalakshmi P. In Silico Molecular Docking of Ocimum sanctum Phytochemicals: Targeting Key Biomarkers in Oral Cancer. Journal of Pharmacy and Bioallied Sciences. 2024; 16(5): S4792-S4799.
39. Natarajan PM, Umapathy VR. Role of transcriptomics in the study of oral cancer. Frontiers in Oral Health. 2025; 6:1524364.
40. Swamikannu B, Umapathy VR, Natarajan PM, Nandini MS, Stylin AGSQ, Vimalarani V, Rajinikanth S. Unlocking the Therapeutic Benefits of Artemisia Annua: A Comprehensive Overview of its Medicinal Properties. Journal of Pharmacy and Bioallied Sciences. 2024; 16(5): S4248-S4253.

41. Yadalam PK, Arumuganainar D, Natarajan PM, Ardila CM. Artificial intelligence-powered prediction of AIM-2 inflammasome sequences using transformers and graph attention networks in periodontal inflammation. Scientific Reports. 2025; 15: 8733.
42. Yadalam PK, Chatterjee S, Natarajan PM, Ardila CM. Comparison of light gradient boosting and logistic regression for interactomic hub genes in Porphyromonas gingivalis and Fusobacterium nucleatum-induced periodontitis with Alzheimer's disease. Frontiers in Oral Health. 2025; 6:1463458.
43. Natarajan PM, Bhuminathan S, Leela B, Bindu K, Loganathan K, Ramachandran V. Smoking and its Role in Oral Cancer. Journal of Pharmacy and Bioallied Sciences 16(5): S4242-S4244.
44. Yadalam PK, Natarajan PM, Ardila CM. Variational graph autoencoder for reconstructed transcriptomic data associated with NLRP3 mediated pyroptosis in periodontitis. Scientific Reports. 2025; 15: 1962.
45. Natarajan PM, Swamikannu B, Sivaraman NM, Stylin AGSQ. Prevention of Oral Cancer: A Comprehensive Guide. Journal of Pharmacy and Bioallied Sciences. 2024; 16(5): S4239-S4241.
46. Pei J, Kumarasamy RV, Jayaraman S, Kanniappan GV, Long Q, Palanisamy CP. Quercetin-functionalized nanomaterials: Innovative therapeutic avenues for Alzheimer's disease management. Ageing Research Reviews. 2025; 104: 102665.
47. Jayaraman S, Prasad M, Natarajan SR, Krishnamoorthy R, Alshuniaber MA, Gatasheh MK, Veeraraghavan VP, Rajagopal P, Palanisamy CP. Molecular mechanisms underlying the effects of beta-sitosterol on TGF-β1/Nrf2/SIRT1/p53-mediated signaling in the kidney of a high-fat diet and sucrose-induced type-2 diabetic rat. Chemico-Biological Interactions. 2025; 411: 111443.
48. Huang Y, Guo H, Liu Y, Jin W, Palanisamy CP, Pei J, Oz F, El-Aty AMA. Effects of Natural Polysaccharides on the Gut Microbiota Related to Human Metabolic Health. Molecular Nutrition & Food Research. 2025; e202400792.
49. Prabhakaran P, Palanisamy CP, Shanmugam A, Damodharan P, Swaminathan H, Devaraj D, Ahalliya RM, Kanniappan GV. Isolation, structural characterization, and molecular docking studies on the bioactive compound from n-Hexane extract of Emilia sonchifolia (L.) DC against the pancreatic cancer target Aurora 2 Kinase. Journal of Complementary and Integrative Medicine. 2024; 22(1): 0290.
50. Jiang H, Kumarasamy RV, Pei J, Raju K, Kanniappan GV, Palanisamy CP. Integrating engineered nanomaterials with extracellular vesicles: Advancing targeted drug delivery and biomedical applications. Frontiers in Nanotechnology. 2024; 6: 1513683.
51. Guo H, Liu Y, Wan T, Song D, Palanisamy CP, Geng J, Pei J, Özmen S, El-Aty AMA. Toward personalized cancer management: Role of precision nutrition–diet interventions. Journal of Functional Foods. 2024; 123: 106584.
52. Natarajan SR, Krishnamoorthy R, Alshuniaber MA, Al-Anazi KM, Farah MA, Rajagopal P, Palanisamy CP, Veeraraghavan VP, Jayaraman S. Identification of FOXM1 as a novel protein biomarker and therapeutic target for colorectal cancer progression: Evidence from immune infiltration and bioinformatic analyses. International Journal of Biological Macromolecules. 282 (Part 4): 137201.
53. Rajendran MS, Jayaraman S, Khan JM, Jasmine S, Prabhakaran RK, Raju MV, Chandrasekaran MK, Ahalliya RM, Kannappan P, Palanisamy CP, Kanniappan GV. Investigating the colon toxicity and carcinogenic role of monosodium glutamate compared with Dimethylhydrazine in male Wistar rats: Exploring the link to childhood colon cancer risk. Journal of King Saud University - Science. 2024; 36(11): 103507.
54. Kumarasamy RV, Natarajan PM, Umapathy VR, Roy JR, Rab SO, Saeed M, Panagal M, Mironescu M, Srinivasan GP, Palanisamy CP. Clinical Applications and Therapeutic Potentials of Advanced Nanoparticles: A Comprehensive Review on Completed Human Clinical Trials. Frontiers in Nanotechnology. 2024; 6:1479993.
55. Jin W, Pei JJ, Roy JR, Jayaraman S, Ahalliya RM, Kanniappan GV, Mironescu M, Palanisamy CP. Comprehensive review on single-cell RNA sequencing: A new frontier in Alzheimer's disease research. Ageing Research Reviews. 2024; 274: 102454.
56. Pei J, Palanisamy CP, Jayaraman S, Natarajan PM, Umapathy VR, Roy JR, Panagal M, Jayaraman S. Curcumin-loaded polymeric nanomaterials as a novel therapeutic strategy for Alzheimer's disease: A comprehensive review. Ageing Research Reviews. 2024; 99: 102393.
57. Pei J, Palanisamy CP, Jayaraman S, Natarajan PM, Umapathy VR, Roy JR, Thalamati D, Ahalliya RM, Kanniappan GV*, Mironescu M. A comprehensive review on starch-based Sustainable Edible Films Loaded with Bioactive Components for Food Packaging. International Journal of Biological macromolecules. 2024; 274 (Part-1): 133332.
58. Palanisamy CP, poompradub S, Sansanaphongpricha K, Subramani K, Sonsudin F. Increased expression levels of PDGF and VEGF magnify the wound healing potential facilitated by biogenic synthesis of silver nanoparticles. Nano-Structures & Nano-Objects. 2024; 39: 101236.
59. Pei J, Palanisamy CP, Jayaraman S, Natarajan PM, Umapathy VR, Roy JR, Thalamati D, Ahalliya RM, Kanniappan GV, Mironescu M. Proteomics Profiling of Extracellular Vesicle for Identification of Potential Biomarkers in Alzheimer's Disease: A Comprehensive Review. Ageing Research Reviews. 2024; 99: 102359.
60. Xi J, Wang T, Xian P, Liu X, Du M, Yang H, Palanisamy CP, Lin W, Long Q. Proteomic insights uncover enhanced neurotherapeutic potential in conditioned mesenchymal stem cell-derived extracellular vesicles. Extracellular Vesicle. 2024; 3: 100037.
61. Pei J, Natarajan PM, Umapathy VR, Swamikannu B, Sivaraman NM, Krishnasamy L, Palanisamy CP. Advancements in the synthesis and functionalization of zinc oxide-based nanomaterials for enhanced oral cancer therapy. Molecules. 2024; 29(11): 2706.

62. Gatasheh MK, Natarajan SR, Krishnamoorthy R, Alsulami TS, Rajagopal P, Palanisamy CP, Veeraraghavan VP, Jayaraman S. Molecular analysis to identify novel potential biomarkers as drug targets in colorectal cancer therapy: an integrated bioinformatics analysis. Molecular and Cellular Oncology. 2024; 11(1): 2326699.
63. Pei J, Yan Y, Jayaraman S, Rajagopal P, Natarajan PM, Umapathy VR, Gopathy S, Roy JR, Sadagopan CS, Thalamati D, Palanisamy CP, Mironescu M. A review on advancements in the application of starch-based nanomaterials in biomedicine: Precision drug delivery and cancer therapy. International Journal of Biological Macromolecules. 2024; 130746.
64. Pei JJ, Yan Y, Palanisamy CP, Jayaraman S, Natarajan PM, Umapathy VR, Gopathy S, Roy JR, Sadagopan JC, Thalamati D, Mironescu M. Materials-based drug delivery approaches: Recent advances and future perspectives. Green Processing and Synthesis. 2024; 13: 20230094.
65. Panneerselvam S, Viswaja K, Deepa E, Prathiba S, Rebecca FS, Nivedha RP, Rajagopal P, Veeraraghavan VP, Sridevi G, Palanisamy CP, Jayaraman S. Hypoglycemic Potential of Acalypha indica in Streptozotocin-Induced Type 2 Diabetic Rats. International Journal of Drug Delivery Technology. 2026; 16(26s):1038-1047.
66. Panneerselvam S, Viswaja K, Prathiba S, Rebecca FS, Nivedha RP, Rajagopal P, Fathima SJH, Veeraraghavan VP, Sridevi G, Palanisamy CP, Jayaraman S. Acalypha Indica Attenuates Insulin Resistance in STZ-Induced Type 2 Diabetic Male Rats: Mechanistic Study. International Journal of Drug Delivery Technology. 2026; 16(26s):1027-1037.
67. Manju NE, Natarajan A, Rebecca FS, Nivedha RP, Hemalatha R, Rajagopal P, Murali R, Veeraraghavan VP, Sridevi G, Palanisamy CP, Jayaraman S. Effect of Seendhil polyherbal formulation in attenuating type-2 diabetes in STZ-induced experimental rats. International Journal of Drug Delivery Technology. 2026; 16(26s):981-989.
68. Manju NE, Natarajan A, Rebecca FS, Nivedha RP, Hemalatha R, Rajagopal P, Murali R, Veeraraghavan VP, Sridevi G, Palanisamy CP, Jayaraman S. Molecular mechanism to identify the effects of Seendhil polyherbal preparation on IRS-1/AKT/GLUT4/NRF2-KEAP-1 mediated signaling in SFZ-induced type-2 diabetic adult male rats. International Journal of Drug Delivery Technology. 2026;16(26s):972-980.
69. Palanisamy CP, Poompradub S, Sansanaphongpricha K, Jayaraman S, Subramani K, Sonsudin F. Biosynthesis of silver nanoparticles (AgNPs) using ethanolic extract of Nigella sativa (L.) seeds promotes wound healing via PDGF and VEGF signalling pathways activation. Biocatalysis and Agricultural Biotechnology. 2023; 54: 102970.
70. Palanisamy CP, Pei JJ, Phaniendra A, Venkata AAN, Jayaraman S, Veeraragahavan VP, Sridevi G, Roy JR, Janaki CS, Thalamati D, Mironescu M, Luo Q, Chai Y, Long Q. New Strategy of Neurodegenerative Disease Treatment with Extracellular Vesicles (EVs) Derived from Mesenchymal Stem Cells (MSCs). Theranostics. 2023; 13(12):4138-4165.
71. Le TDH, Tuan HNA, Nguyen VT, Le AT. Hydroxyapatite− loaded starch/polyvinyl alcohol scaffold for bone regeneration application: preparation and characterization. Journal of Sol-Gel Science and Technology. 2023;107(2):441-51.
72. Ramezani M, Ripin ZM. An overview of enhancing the performance of medical implants with nanocomposites. Journal of Composites Science. 2023;7(5):199.
73. Shafaat S, Hussain N, Asif M, Abbasi Z, Khan H, Iqbal M, et al. Understanding adsorption phenomena through dynamic light scattering and stability measurements. International Journal of Environmental Analytical Chemistry. 2025:1-22.
74. Su J, Yang M, He Z, Guan Y, Fu S. The effect of particle size and dispersity index on the drying behavior of colloidal microdroplets. Colloids and Surfaces A: Physicochemical and Engineering Aspects. 2025;708:135965.
75. Pochapski DJ, Carvalho dos Santos C, Leite GW, Pulcinelli SH, Santilli CV. Zeta potential and colloidal stability predictions for inorganic nanoparticle dispersions: Effects of experimental conditions and electrokinetic models on the interpretation of results. Langmuir. 2021;37(45):13379-89.
76. Pedroso-Santana S, Fleitas-Salazar N. The use of capping agents in the stabilization and functionalization of metallic nanoparticles for biomedical applications. Particle & Particle Systems Characterization. 2023;40(2):2200146.
77. Chahardoli A, Haghighi ZMS, Shokoohinia Y, Fattahi A. Plant based biosynthesis of TiO2NPs and evaluation of their cytotoxicity, antihemolytic, and protein antidenaturation effects. South African Journal of Botany. 2023;163:37-44.
78. Al-Dulaimy WYM, Hussein AA, Mahdi MA, Kadhom M. In Vitro Inhibition of Xanthine Oxidase Purified from Arthritis Serum Patients by Nanocurcumin and Artemisinin Active Compounds. Molecules. 2023;28(13):5124.